Contribution to the Development of Cylindrical Gears

Gorazd Hlebanja and Jože Hlebanja

Abstract Authors propose S-gears as an improvement with regard to involute gears. The tooth flank profile of the former is based on the basic rack profile, defined as an analytic curve and implies the shape of a tooth flank which is the matter of discussion in the paper. An important feature of S-gears is the convex-concave contact of a pinion and a gear in the meshing start and meshing end areas which provides better characteristic as in E-gears. Therefore, the mechanism of sliding, the oil film build-up and power losses will be demonstrated. In this context several important features, e.g. curvatures, Hertzian stresses, temperatures, oil film thickness, velocity circumstances will be also discussed. The S-type gears can be used in all scales from small to large and in planetary gear trains as well.

Keywords Cylindrical gears · Non-involute gear geometry · Gear contact · Meshing circumstances

List of Symbols

P_i	Point on the rack profile
G_i	Point on a gear tooth flank
U_i	Point on the path of contact
x, y	Cartesian coordinates
a_p	Size factor
n	Exponent
t_{Pi}, t_{Gi}	Tangents in point P_i, G_i
α_C	Pressure angle
α_{Gi}	Inclination angle in G_i

G. Hlebanja (✉) · J. Hlebanja
University of Ljubljana, Ljubljana, Slovenia
e-mail: gorazd.hlebanja@fs.uni-lj.si

J. Hlebanja
e-mail: joze.hlebanja@siol.net

G. Dobre (ed.), *Power Transmissions*,
Mechanisms and Machine Science 13, DOI: 10.1007/978-94-007-6558-0_23,

ρ_{Gi}	Radius of curvature in G_i
m	Module
ρ_1, ρ_1	Radii of curvature—gear 1, gear 2
ρ_{red}	Reduced radius of curvature
F_t	Tangential force
F_b	Contact force
α_U	Incidence angle
b	Gear width
E	Modulus of elasticity
v	Poisson's ratio
σ_H	Hertzian stress
$\mathbf{v_p}$, $\mathbf{v_s}$	Absolute velocity—gear, pinion
$\mathbf{v_{rP}}$, $\mathbf{v_{rS}}$	Relative velocity—gear, pinion
$\mathbf{v_{At}}$	Tangential velocity along the path of contact
$\mathbf{v_g}$	Sliding velocity
$\mathbf{v_t}$	Tangential velocity
φ_{UP}, φ_{US}	Angular position—gear, pinion
ω_P, ω_S	Angular velocity—gear, pinion
$\vartheta_{fl}\vartheta_M$	Flash, mass temperature
μ	Friction coefficient
w_{tb}	Line load
E'	Reduced Young's modulus
v	Poisson's ratio
λ	Thermal conductivity
ρ	Density
c	Specific heat
h_0	Minimal oil film thickness
u	Average contact velocity
η_0	Dynamic viscosity (atm. circumstances)
α	Pressure viscosity coefficient
κ	Ellipcity parameter (a, b—ellipse semi-axes)

1 Introduction

Gears are frequent choice for power transmission from fast power sources to working machines. Transmitted power levels can vary from low in miniature mechanisms to very high in contemporary wind power plants. Power ranges can exceed 5 MW in the latter.

Transmission gears from the engine to the drive wheels are also of great importance in the automotive and truck industry. The overwhelming majority of gears used in practice are involute. User requirements are increasing, therefore the

gears should provide more accurate transfer of motion, better endurance, higher efficiency and the lowest dimensions, which are nowadays the major trends in gear development, which should be followed by both, the researchers and gear manufacturers, as reported by Blickle (2010), Hirt (2010), Joachum et al. (2010).

The involute gear shape has been in use from the time of Euler and is based on the mathematical form of the involute function. The involute tooth flank can be put through the kinematic velocity pole which furthermore resides on the kinematic circle and divides the tooth flank to the addendum and dedendum part.

The active length of the tooth dedendum of the involute gear is relatively short; the corresponding curvature radius in the direction of involute starting point is decreasing to zero. Very high contact loads and sliding arise in this area due to power transmission from a pinion to a gear, which cause energy losses because of friction and consequently severe damages of teeth flanks in form of wear, micro and macro pitting as stated by Butterfield (2010) and Lütig (2007) in his dissertation. S-gears exhibit more appropriate shape of tooth flank profile, with higher loading capacity and lower energy losses in power transmission.

S-gears are illustrated in Fig. 1. The tooth flank profile is based on the basic rack profile as proposed by Hlebanja (2010). The rack profile is defined as an analytic curve, Eq. (1), for which the derivatives are also defined.

$$y_{Pi} = a_p(1 - (1 - x_{Pi})^n) \tag{1}$$

where (x_{Pi}, y_{Pi}) are Cartesian coordinates originating in the pitch point C, a_p parameter designating a size factor (in this case with the value $a_p = 1{,}30{,}267$), and n is the exponent ($n = 1{,}9$). Both, a_p and n, have decisive influence on expected

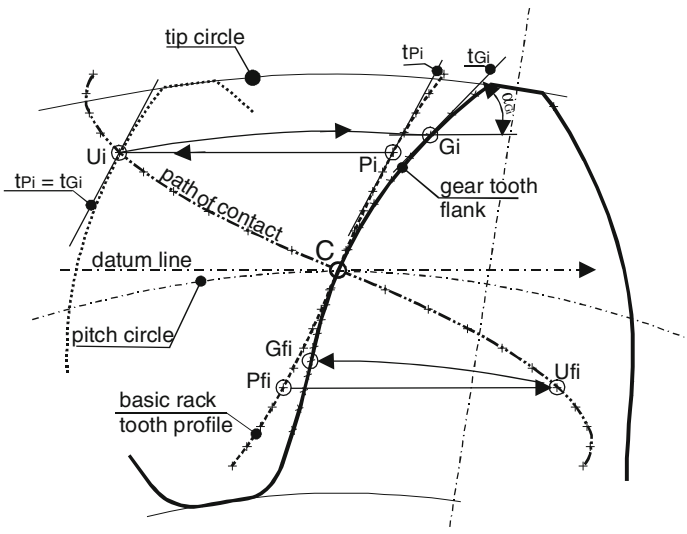

Fig. 1 S-gear tooth flank profile creation

characteristics of the designed gears. Equation (1) defines the addendum part of the rack profile and the half symmetric counterpart defines its dedendum part.

Furthermore, the tangent t_{Pi} is defined for any point P_i on the rack profile. Point U_i on the path of contact is defined based on t_{Pi}. U_i can be regarded as a rack's cutting edge generating a gear tooth flank profile point G_i.

The rack tooth flank distance from the velocity pole C in point U_i is P_iU_i, which is exactly the arc U_iG_i length on the reference circle for which the emerging gear point G_i rotates around its axis. The transformations from P_i to U_i and from U_i to G_i are unique and reversible, that is bijective. The path of contact is characterized by its half symmetry. Properties of S-gears can be illustrated by mating gear and pinion shown in Fig. 2. The dedendum of one gear is in contact with the addendum of the other gear during mating which corresponds to a half of the path of contact, which is unique for a given module regardless of the number of teeth. An important feature of S-gears is a convex-concave contact of a pinion and a gear in the meshing start and end areas (in vicinity of points A and E). Another advantage is minimal teeth number of S-gears, which can be as low as four.

S-type rack differs from involute rack by parabolic shaped flanks. With the defined rack the same manufacturing technology can be employed in S-gears as in involute case, however always with appropriate cutting profiles.

Regarding the geometric shape S-gears are usable for small and micro gears in miniature applications (Hlebanja 2011) as well as for large gears, suitable for high power transmission.

Details of geometric definitions and manufacturing principles of S-gears have been disclosed in several recent papers (e.g. Hlebanja 2010, 2011). Therefore, several important characteristics of S-gears will be revealed and discussed in the continuation, which prove their advantages, not only in spur gears, but also in

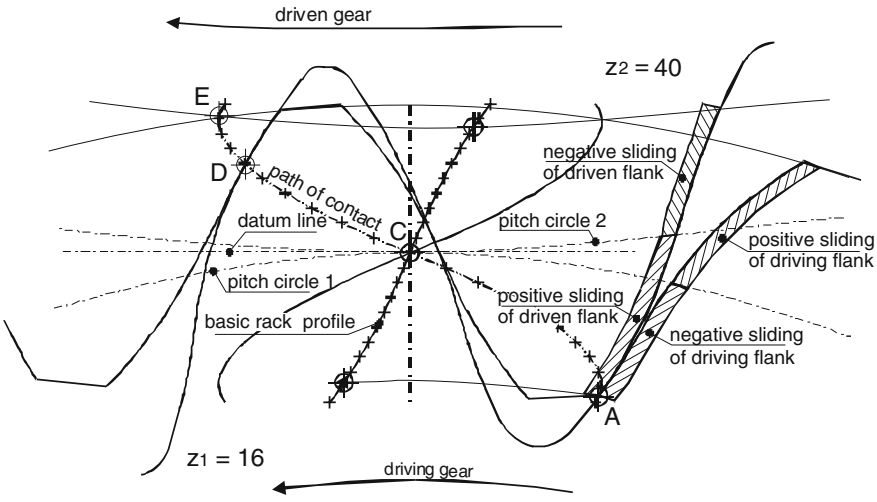

Fig. 2 Meshing circumstances and sliding zones

helical and skew gears as well. S-gear geometry is also appropriate in internal gears, thus enabling design of planetary gear trains.

2 Important Characteristics

2.1 Tooth Flank Curvature

The tooth flank profile is defined continuously for any point, based on the previously explained transformations from the rack profile to the path of contact and at last to the gear tooth flank. Its curvature is mathematically defined by an expression containing first and second derivative. Knowing tooth profile inclination angle for any point of the profile implies tangent and thus first and second derivative in that point (Hlebanja 2010). The curvature is therefore given by a simple Eq. (2)

$$\rho_{Gi} = \frac{1}{\cos \alpha_{Gi}} \cdot m. \tag{2}$$

Characteristic of the meshing gears is that both gears dedendum flanks are partly concave, the rest being convex, whereas both addendum flanks are convex. Both flanks are convex around the pitch point, with relative high radii of curvature. Another important observation is that a concave-convex contact appears in the vicinity of meshing start and meshing end areas, which implies better loading circumstances there.

In order to evaluate tooth flank durability in a contact point the reduced radii of curvature ρ_{red} are necessary

$$\rho_{red} = \frac{\rho_1 \rho_2}{\rho_1 \pm \rho_2} \tag{3}$$

If the contact between two flanks is convex–convex, both factors of the denominator should be summed, otherwise (convex-concave case) they should be subtracted.

Distribution of the reduced radii of curvature over the path of contact diagrammatically represented in Fig. 3, reveals some interesting facts. First, comparatively high values of ρ_{red} are in the zones AB and DE are due to convex-concave contact, indicating that the contact load is smaller and lubrication conditions are better; quite so two pairs of teeth are in contact in AB and DE. ρ_{red} changes are small and have a local maximum in the pitch point in the zone of the single pair contact BCD, which indicates evenly distributed power transmission. The actual curve depends on geometrical data (number of teeth, module) of a gear pair and the value in C equals that in involute gear shape.

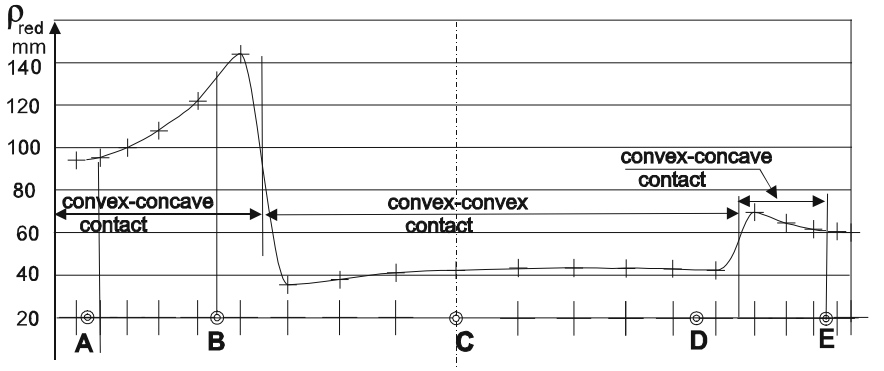

Fig. 3 Reduced radii of curvature along the path of contact $m = 30$ mm, $z_1 = 42$ and $z_2 = 12$

2.2 Contact Force and Hertzian Pressure

The dedendum part of a tooth flank is the most loaded area in power transmission from a gear to a pinion, due to negative sliding in that area. This is why this loading state is of particular importance and discussed in the following paragraphs. Contact load in a particular time instant appears in the contact spot on the path of contact and is influenced by the contact force F_b, which is acting rectangular to the teeth flanks in the direction of the kinematic pole C. The situation is illustrated in Fig. 4 particularly for contact point B. The contact force magnitude along the path of contact is variable conforming to the incidence angle α_U changes, as indicated in Fig. 5, and defined by following equation

$$F_b = \frac{F_t}{\cos \alpha_U} \tag{4}$$

Hertzian pressure as a common measure of contact load of mating teeth flanks is expressed by

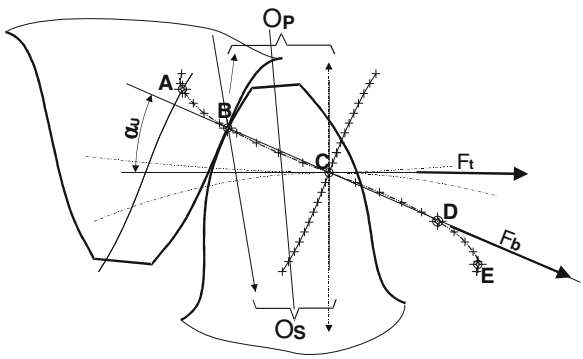

Fig. 4 Forces resulting on teeth flanks

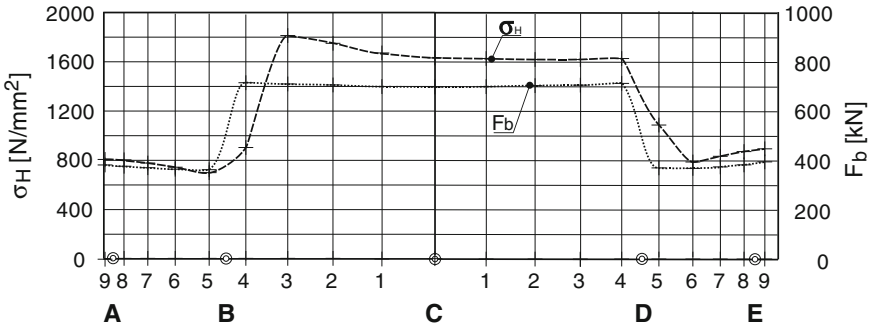

Fig. 5 Hertzian pressure and contact force along the path of contact $m = 30$ mm; $b \approx 6{,}7\ m = 200$ mm; $E = 2{,}06 \times 10^6$ N/mm^2; $\nu = 0{,}3$

$$\sigma_H = \sqrt{\frac{F_b E}{2\pi b \rho_{red}(1-\nu^2)}} \leq \sigma_{Hdop}. \tag{5}$$

However, Hertzian pressure may not exceed maximal allowable limit σ_{Hdop}. The contact force F_b, tooth width b and reduced radius of curvature ρ_{red} in Eq. (5) are those design parameters which decisively influence gear durability. The tangential force F_t, transmitted from the driving to the driven gear, is distributed among two gear pairs in the zones of double contact AB and DE. This is also true for F_b, which is clearly indicated in the diagram, Fig. 5.

2.3 Velocity Circumstances

Velocity circumstances in the gear tooth contact points, appearing along the path of contact, decisively influence oil film thickness. They depend on the tooth flank geometry derived from the path of contact, whereas each point on the tooth flank profile features a unique curvature radius. Absolute velocities, relative velocities of teeth flanks, and the contact point movement velocity in the tangential direction to the path of contact can be distinguished with regard to the tangential direction to the teeth flanks in the contact point. Two critical states are illustrated in Fig. 6, namely first in the vicinity of the meshing start and then in the vicinity of the meshing end. The absolute velocity of the pinion tooth flank is represented by the vector $\mathbf{v_s}$, and the absolute velocity of the gear by $\mathbf{v_P}$. The relative velocities $\mathbf{v_{rS}}$ and $\mathbf{v_{rP}}$ act tangentially to corresponding teeth flanks, whereas $\mathbf{v_{At}}$ is the velocity of the contact point in the direction of tangent to the path of contact. Thus, expressions for $\mathbf{v_s}$ and $\mathbf{v_P}$ are

$$\vec{v}_S = \vec{\omega}_S \times \vec{r}_S \ \text{ and } \ \vec{v}_P = \vec{\omega}_P \times \vec{r}_P \tag{6}$$

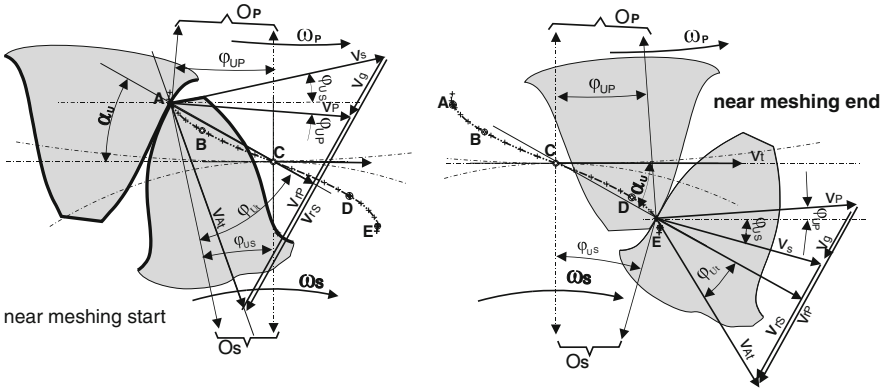

Fig. 6 Velocity circumstances for S-gears *left*—in the meshing start area; *right*—in the meshing end area

Velocity components in the direction of teeth flank surfaces influence the oil film formation; the corresponding velocity of the pinion $\mathbf{v_{rS}}$ and the gear $\mathbf{v_{rP}}$ are

$$\vec{v}_{rS} = \vec{v}_S - \vec{v}_{At} \text{ and } \vec{v}_{rP} = \vec{v}_P - \vec{v}_{At} \tag{7}$$

The sliding velocity $\mathbf{v_g}$ is defined as the difference of absolute velocities of teeth flanks in the contact point or as the difference of both relative velocities.

$$\vec{v}_g = \vec{v}_S - \vec{v}_P \text{ and } \vec{v}_g = \vec{v}_{rS} - \vec{v}_{rP} \tag{8}$$

Values of both relative velocities can be calculated from geometric relations.

$$\begin{aligned} v_{rP} &= v_P \sin(\alpha_{Ui} - \varphi_{UP}) + v_t \cos\alpha_{Ui} \tan\varphi_{Ui} \\ v_{rS} &= v_S \sin(\alpha_{Ui} - \varphi_{US}) + v_t \cos\alpha_{Ui} \tan\varphi_{Ui} \end{aligned} \tag{9}$$

The diagram Fig. 7 illustrates functional dependence of relative velocities of the path of contact and these particular calculations assume the tangential velocity amounting to 2,26 m/s.

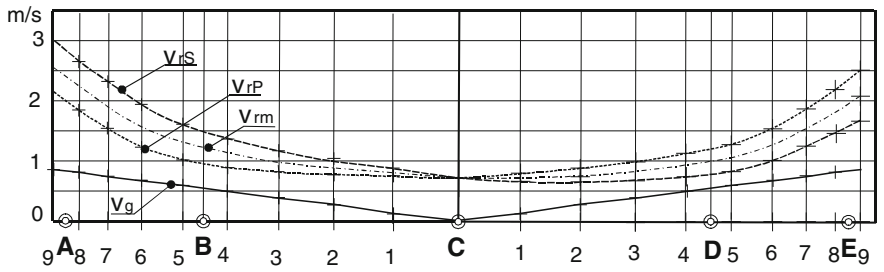

Fig. 7 Diagram of the relative velocities along the path of contact v_{rm} is aritmetic average of v_{rS} and v_{rP}

2.4 Temperatures of Teeth Flanks in a Contact Spot

The contact temperature is a function of the gear bulk material temperature ϑ_M and the flash temperature ϑ_{fl}. The first is a a steady temperature during operation, and the latter is an instantaneous temperature of the contact appearing due to local friction heat and reaches its maximal value at the gear meshing point—contact; afterwards it diminishes. The apparent time of the contact depends on angular velocities of gears, on actual geometry and surface parameters, it is exceedingly short in general and thus its temperature contribution is named flash temperature. The flash temperature is an important influencing factor in emergence of scuffing and to great extent also of micro-pitting. If angular velocities are rather low then no high temperature shocks should be expected. The flash temperature functional dependence on the path of contact is illustrated in diagram, Fig. 8. The Block's expression for the line contact (Blok 1963 and Theyse 1967) was employed in calculations:

$$\vartheta_{fl} = 0,62\mu(w_{tb})^{0,75}\left(\frac{E'}{\rho_{red}}\right)^{0,25}\frac{v_g}{\sqrt{B_{MS}v_{rS}}+\sqrt{B_{MP}v_{rP}}} \tag{10}$$

where $E' = E/(1\text{-}\nu^2)$ and $\sqrt{B_{MS,P}} = \sqrt{\lambda\rho c} = 12,5\left[\mathrm{N/mms^{0,5}K}\right]$. The heat contact coefficient is material property—the above value is for steel. The other values are $\lambda = 47,5[\mathrm{W/(mK)}]$, $\rho = 7800\,[\mathrm{kg/m^3}]$, $\mathrm{c} = 440\,[\mathrm{J/(kgK)}]$. An average value for the friction coefficient results from data (Nieman and Winter 1989) and amounts to 0,08. All other variables are varying along the path of contact and represented in preceding figures. The diagram represented in Fig. 8 indicates that thermal load of the teeth flanks in the zones of double contact is comparable smaller as in the zone of single contact. This is due to lower teeth load and higher reduced radii of curvature, whereas in the single contact zone the flash temperature diminishes towards C, where its value is 0, which is due to lowering of the sliding velocity.

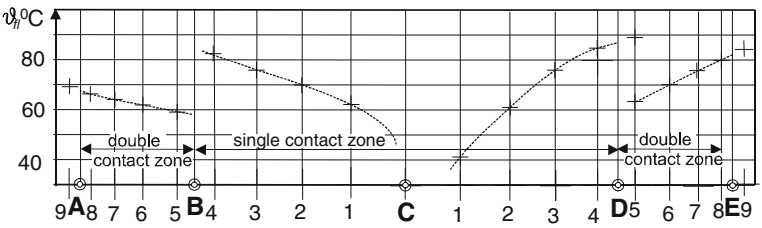

Fig. 8 Flash temperature along the path of contact (the bulk temperature should be added to the above values)

2.5 Oil Film Thickness

Micro-pitting is fatigue damage of gear teeth flanks where the contact area is surface-hardened and ground. Emerging micro-damages, lowering transmission accuracy, evolve into gearing failures. The main cause of micro-pitting is attributed to insufficient lubrication of the contact surfaces due to slow sliding speeds and high contact loads—i.e. slow running gears is mixed lubrication (Stachowiak and Batchelor 2006, p. 311). Therefore, the oil film thickness between the meshing gear flanks is one of crucial parameters in this context and it should be higher as roughness. The oil film thickness is influenced by: load, contacting teeth flank surfaces velocities, sliding velocities, temperature, surface roughness, oil characteristics, material properties, and tooth shape which actually transmits the load. Another important factor is friction heat governing oil temperature which affects its viscosity. Dimensioning of gears with regard to micro-pitting is based on oil film thickness based on elasto-hydrodynamic lubrication theory. Due to EHL importance, research led to many improvements. However, most of them derive from Dawson's and Higginson's (1977) work. Following equation (Stachowiak and Batchelor 2006) was used for a general elliptic type of contact in order to get basic relations:

$$\frac{h_0}{\rho_{red}} = 3,63\left(\frac{u\,\eta_0}{E'\,\rho_{red}}\right)^{0,68}(\alpha E')^{0,49}\left(\frac{F_b}{E'\rho_{red}^2}\right)^{-0,073}\left(1 - 0,61e^{-0,68\kappa}\right). \quad (11)$$

Since the contact surfaces, dealt with here, are cylindrical their contact is the line contact. Therefore, the longer ellipse axis limits to infinity, so the ellipticity parameter value is 0. Assuming equilibrium bulk thermal circumstances and given material, Eq. (11) can be rearranged to

$$h_0 = \left[3,63\eta_0^{0,68}\alpha^{0,49}E'^{-0,117}\right]u^{0,68}\rho'^{0,466}W^{-0,073}. \quad (12)$$

Variables in Eq. (12) are the average contact velocity, the reduced radius of curvature and the contact force, whereas the values in brackets are constant for given conditions. The oil viscosity parameters in calculations are from Stachowiak and Batchelor (2006, p. 21). Heavy industrial oil was selected having high dynamic viscosity and the pressure viscosity coefficient values collected in Table 1. The reduced elasticity module for steel amounts to 206×10^9 N/m^2.

Knowing above data and functional values for the average velocity (Fig. 7), the contact force (Fig. 5) and the reduced radius of curvature along the path of contact (Fig. 3), a diagram, Fig. 9, can be drawn. The curve in the diagram has been

Table 1 Viscosity parameters for a heavy industrial oil

ϑ	30 °C	60 °C
$\eta 0$	153×10^{-3} Pa	34×10^{-3} Pa
α	$23,7 \times 10^{-9}$ m^2/N	$20,5 \times 10^{-9}$ m^2/N

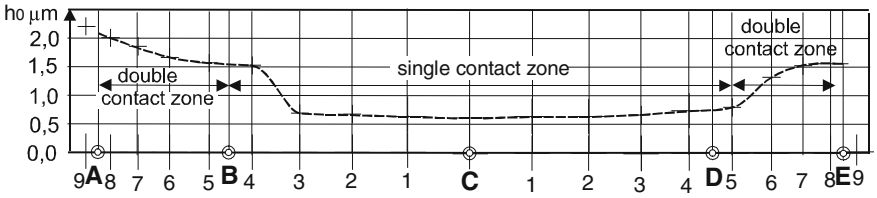

Fig. 9 Oil film thickness course along the path of contact

calculated for operating conditions with the temperature 30 °C. The oil film thickness lowers for about 33.6 % when the temperature is 60 °C. Thus, the minimal oil thickness in the kinematic pole C is 0.21 µm. This is the same value as the value in C for involute gears with the same module and the same gear ratio. Oil film thickness enlarges considerably in double contact zones near both end contact zones.

Considering, that the potential danger of micro-pitting exist in the zone of meshing start for involute gears (Höhn et al. 2003), S-gears exhibit advantage in this context due to the tick oil film in this area, which diminishes possibility of damage.

3 Conclusion

Solutions for preventing or diminishing micro-pitting occurence are prevailingly searched for in the direction of better lubrication means, in high quality surface treatment (super-finishing), in gear tooth flank profile change in meshing start area, and finally in better materials. This proposal introduces a new gear tooth flank profile—S-gear tooth flank profile, which assures higher comparative curvature radii, and thus lower contact load and higher relative velocities of the contact surfaces which implies better lubrication.

Not only that the curvature radii are higher, the mating gears exhibit convex-concave contact in the vicinity of the contact start and contact end, whereas slowly varying curvature is characteristic for the central area.

Due to their S-shape, the velocity characteristics of mating gears are improved, especially in both external areas with high relative velocities and low sliding velocity.

The meshing start zone in involute gears represents potential danger of micro-pitting, whereas S-gears exhibit advantage in this context due to the tick oil film in this area, which diminishes possibility of damage.

S-gears can be used in a large and small scale application and planetary gear trains. Comparatively smaller outer diameter of internal S-gears also implies smaller weight.

It is true that special tools are necessary to produce S-gears, however with contemporary CNC machine tools and technologies this does not denote much of an obstacle.

References

Blickle R (2010) SEW: crisis scenarios are driving forces for innovation and progress. In: International conference on gears, Munich, 4–6 Oct 2010

Blok H (1963) The flash temperature concept. Wear 6:483–494

Butterfield S (2010) Wind turbine micro-pitting workshop. Technical report NREL/TR 500-46572, February 2010

Dowson D, Higginson GR (1977) Elasto-hydrodynamic lubrication. SI Edition. Pergamon Press, Oxford

Hirt M (2010) What are the influences of the global financial and economic crisis on the transmission and gear market worldwide. In: International conference on gears, Munich, 4–6 Oct 2010

Hlebanja J, Hlebanja G (2010) Spur gears with a curved path of contact for small gearing dimensions. VDI Berichte 2108:1281

Hlebanja G (2011) Specially shaped spur gears: a step towards use in miniature mechatronic applications. In: 7th International science conference on research and development of mechanical elements and systems—IRMES 2011, April 27–28. Zlatibor, Serbia. Proceedings. Niš: Mechanical Engineering Faculty, pp 475–480

Höhn BR, Oster P, Steingröver G (2003) The new micro-pitting short test 1. In: International conference power transmissions'03, Varna, Bulgaria, 11–12 Sept 2003

Joachum F-J, Börner F-J, Kurz N (2010) How to minimize power losses, transmissions, axles and steering systems. VDI-Berichte 2108:111

Lütig G (2007) Großgetriebe-Graufleckigkeit, Dissertation. Universität Bochum, Bochum

Nieman G, Winter H (1989) Maschinenelemente, Band II: Getriebe allgemein, Zahn-rad-getriebe Grundlagen, Stirnrad Getriebe. ISBN 3-540-11149-2, Springer Berlin, Heidelberg, New York

Stachowiak GW, Batchelor AW (2006) Engineering tribology. Elsevier Butterworth-Heinemann, Oxford

Theyse FH (1967) Die Blitztemperaturhypothese nach Blok und ihre praktische Anwendung bei Zahnrädern. Schmiertechnik 14:22–29